Sonochemical and Microwave-Assisted Preparations of PbTe and PbSe. A Comparative Study

R. Kerner, O. Palchik, and A. Gedanken*

Department of Chemistry, Bar-Ilan University, Ramat-Gan, Israel 52900

Received December 20, 2000

Sonochemical and microwave-assisted polyol reduction methods were used to prepare PbSe and PbTe. Products prepared by both methods were compared and analyzed by XRD, EDX, TEM, HR-TEM, elemental analysis, FT-IR, and thermal methods (DSC and TGA). In both methods almost pure lead chalcogenide phases were prepared, which were almost free of carbon (<0.08%), but the morphology of the resultant nanoparticles was entirely different. The mechanism of formation for the lead chalcogenide nanoparticles for both microwave and sonochemical reactions is discussed.

Introduction

Tellurides and selenides have attracted considerable interest because of their intriguing properties and structural diversity.[1−3] They find applications in fields such as semiconducting devices, thermoelectricity, and optoelectronics.[4−8] In recent years a growth in publications related to the applications of the selenides and tellurides is accounted. Emphasis has been devoted to their preparation in the nanophased form. This is due to the modern trend of miniaturization, on one hand, and to the unique properties associated with the nanostructure, on the other. Unfortunately, there is an immense delay in the development of synthetic methods for the preparation of these compounds. Several methods have been known for the preparation of chalcogenides. They are as follows: (1) gas-phase reaction between elements or compounds and gaseous H_2Se and H_2Te, (2) solid-state reactions, (3) chemical bath deposition and precipitation, and (4) pyrolysis of single source precursors.[9−14] Generally, all these reactions require high temperatures (∼500 °C) and/or the use of toxic and highly sensitive precursors. From our point of view one of the most promising methods applicable to the synthesis of the nanoparticles is the solvothermal technique. Unlike most other synthetic processes, the solvothermal synthesis involves much milder conditions and softer chemistry conducted at relatively lower temperatures.[15] This technique (especially the hydrothermal method) is widely employed for the crystal growth of many inorganic compounds.[16,17] An intriguing achievement of this synthetic technique includes the preparation of new phases, inaccessible at high temperatures, because of their thermodynamic metastability.[3] Recently, a few reports have described the preparation of metallic and main group chalcogenides under solvothermal conditions using ethylenediamine as a solvent.[18−25] These reaction are conducted in autoclaves, with temperatures kept in the range of 120−200 °C and requiring relatively high pressures. Among the disadvantages of the solvothermal reaction we can mention the high pressure, the prolonged reaction time (from few hours to the days), and the solvent incorporation into the product.[26]

In exploring the solvothermal method as a route for the synthesis of metal chalcogenides, we have chosen ethylene glycol as a solvent. Reactions were conducted using either microwave heating or sonochemistry for the

* To whom correspondence should be addressed. E-mail: gedanken@mail.biu.ac.il.

(1) Knockaert, G. In *Ullmann's Encyclopedia of Industrial Chemistry*; VCH: Weinheim, 1995; Vol. A26, p 177.
(2) Nimitz, G.; Schlicht, B. *Narrow-Gap Semiconductors*; Springer-Verlag: New York, 1985.
(3) Sheldrick, W. S.; Wachhold, M. *Angew. Chem., Int. Ed. Engl.* **1997**, *36*.
(4) Rowe, D. M., Ed. *CRC Handbook of Thermoelectrics*; CRC Press Inc.: New York, 1995.
(5) Chung, D. Y.; Hogan, T.; Brazis, P.; Rocci-Lane, M.; Kannewurf, C.; Bastea, M.; Uher, C.; Kanatzidis, M. G. *Science* **2000**, *287*, 1024.
(6) Masek, J.; Maissen, C.; Zong, H.; Platz, W.; Reidel: H.; Koniger, M.; Lambrecht, A.; Tacke, M. *Nucl. Instrum. Method A* **1990**, *288*, 104.
(7) Prier, H. *Appl. Phys.* **1979**, *20*, 189.
(8) Zogg, H.; Fach, A.; John, J.; Masek, J.; Muller, P.; Paglino, C.; Bottler, W. *Opt. Eng.* **1994**, *33*, 1440.
(9) Roof, L. C.; Kolis, J. W. *Chem. Rev.* **1993**, *93*, 1037.
(10) Kanatzidis, M. *Chem. Mater.* **1990**, *2*, 353.
(11) Kanatzidis, M. G.; Sutoric, A. C. *Prog. Inorg. Chem.* **1995**, *43*, 151.
(12) Coustal, R. *J. Chem. Phys.* **1958**, *38*, 277.
(13) Wang, W.; Geng, Y.; Qian, Y.; Ji, M.; Liu, X. *Adv. Mater.* **1998**, *10*, 1479.
(14) Henshaw, G.; Parkin, I. P.; Shaw, G. *Chem. Commun.* **1996**, 1095.
(15) Demazeau, G. *J. Mater. Chem.* **1999**, *9*, 15.
(16) Barrer, R. M. *Hydrothermal Chemistry of Zeolites*; Academic Press: London, 1982.
(17) Rabenau, A. *Angew. Chem., Int. Ed. Engl.* **1985**, *24*, 1026.
(18) Das, B. K.; Kanatzidis, M. G. *J. Organomet. Chem.* **1996**, *513*, 1.
(19) Li, B.; Xie, Y.; Huang, J. X.; Su, H. L.; Qian, Y. T. *J. Solid State Chem.* **1999**, *146*, 47.
(20) Xie, Y.; Li, B.; Su, H. L.; Liu, X. M.; Qian, Y. T. *Nanostruct. Mater.* **1999**, *11*, 539.
(21) Yang, J.; Yu, S. H.; Yang, X. L.; Qian, Y. T. *Chem. Lett.* **1999**, 839.
(22) Yu, S. H.; Yang, J.; Wu, Y. S.; Han, Z. H.; Lu, J.; Xie, Y.; Qian, Y. T. *J. Mater. Chem.* **1998**, *8*, 1949.
(23) Li, B.; Xie, Y.; Huang, J.; Qian Y. *Ultrason. Sonochem.* **1999**, *6*, 217.
(24) Zhan, J. H.; Yang, X. G.; Wang, D. W.; Xie, Y.; Qian, Y. T. *Inorg. Chem. Commun.* **1999**, *2*, 447.
(25) Zhu, J. J.; Palchik, O.; Chen, S. G.; Gedanken, A. *J. Phys. Chem. B* **2000**, *104*, 7344.
(26) Li, J.; Chen, Z.; Wang, R.-J.; Prospero, D. M. *Coord. Chem. Rev.* **1999**, *190−192*, 707.

10.1021/cm001411h CCC: $20.00
Published on Web 03/16/2001

activation (of these reactions). In the 1980s, Fievet et al. used ethylene glycol as a solvent and reducing agent for the preparation of submicrometer particles of the transition metals. This method is known as the *polyol* process.[27−31] The mechanism of this reaction is still only poorly understood. It is, however, known that the reduction is based on the decomposition of the ethylene glycol and its conversion to diacetyl. Recently, Tarascon and co-workers demonstrated that in these reactions the temperature is a dominant factor in affecting the reactivity. The temperature itself influences three factors: (1) Reduction potential of ethylene glycol; (2) rupture and creation of chemical bonds; (3) diffusion.[32] All these factors make the microwave heating and sonochemistry techniques favorable methods for the fabrication of chalcogenides using ethylene glycol as a solvent. These techniques are specially known as high-temperature activating methods. To the best of our knowledge, this is the first time that the polyol process is reported as being used for the preparation of the main group telluride and selenide materials. The two methods chosen for this reaction have different modes of operation. In the case of microwave irradiation there are two main modes of action. The first occurring in the liquid phase is a coupling between the oscillating electric field (2.45×10^9 Hz) and the permanent dipole moment of the molecule resulting in molecular rotations, which bring to rapid volumetric heating of the liquid phase. The ethylene glycol is an excellent susceptor of the microwave radiation because of its high permanent dipole. In the second mode, metallic particles, produced as intermediates in the polyol reaction, are also good susceptors of the microwave radiation and cause the rapid heating of these particles. The temperature in the reaction container will therefore be much higher than the surrounding liquid. In addition to being an excellent susceptor of the microwave radiation, ethylene glycol serves also as a solvent. Mingos and Whittaker[33] have recently shown that high boiling point alcohols are superior solvents in microwave-assisted reactions because of their property of preventing arching. The arching is known to lead to the decomposition of solvents in the microwave-assisted reactions, yielding carbon and carbonaceous residues. Arching is considered the main cause for the high level of impurities in the end product.

The chemical effect of ultrasound arises from acoustic cavitation, that is, the formation, growth, and implosive collapse of bubbles created in a liquid. The implosive collapse of the bubbles generates a localized hot spot through adiabatic compression or shock wave formation within the gas phase of the collapsing bubble. The conditions formed after the collapse of the bubble have been experimentally determined, resulting in a transient temperature of ~5000 K, pressure of 1800 atm, and cooling rate in excess of 10^{10} K/s. The equation dictating the conditions resulting from the adiabatic implosion show that the final temperature is inversely proportional to the vapor pressure inside the collapsing bubble. In the case of nonvolatile solutes the only gas inside the collapsing bubble will be the solvent vapors. Taking this into consideration will make ethylene glycol an excellent solvent for sonochemistry. On the other hand, the development of a bubble to its full size is strongly dependent on the viscosity of the solvent. Ethylene glycol in this respect is not a favorable solvent for sonochemistry.[34]

In the current report we compare the influence of the microwave irradiation and ultrasound methods in the polyol synthesis of PbSe and PbTe.

Experimental Section

All reagents were of highest purity. Elemental Te, Se, lead acetate, and ethylene glycol were all purchased from Aldrich Co. and used without further purification. The X-ray diffraction patterns of the products were recorded by employing a Bruker AXS D8 advance powder X-ray diffractometer (using Cu Kα $\lambda = 1.5418$ Å radiation). EDX measurements were conducted using an X-ray microanalyzer (Oxford Scientific) built on a JSM-840 scanning electron microscope (JEOL). The transmission electron micrographs (TEM) were obtained by employing a JEOL-JEM 100SX microscope, working at 100-kV accelerating voltage. High-resolution TEM (HRTEM) images were obtained by employing JEOL-3010 with 300-kV accelerating voltage. A conventional CCD camera, with resolution of 768×512 pixels, was used to digitize the micrographs. Image processing of these digital images was performed using Digital Micrograph software. HRTEM image calculation and electron diffraction indexing were performed using the EMS package.[35] Samples for TEM were prepared by placing a drop of the sample suspension on a copper grid (400 mesh, electron microscopy sciences) coated with carbon film and were allowed to dry in air. Elemental analysis (carbon) was done by employing an EA 1110 CHNS-O instrument. The differential scanning calorimetric analysis (DSC) was carried out on a Mettler Toledo TC 15, using nitrogen or argon gas as a purging gas; the scanning rate was 5 °C/min. The IR spectra were recorded on a Nicolet Impact 410 FTIR spectrometer using KBr pellets.

Ultrasonic irradiation was accomplished with a high-intensity ultrasonic probe (Misonix, XL Sonifier, 1.13-cm diameter; Ti horn, 20 kHz, 60 W cm^{-2}) immersed directly in the reaction solution. Microwave-assisted reactions were conducted in the Spectra-900 W, 2.45×10^9 Hz working frequency, domestic microwave oven, modified with a refluxing system. In all experiments the microwave oven worked in the following cycling mode: on for 16 s, off for 4 s, the total power always 900 W. This cycling mode was chosen to prevent violent "bump" boiling of the solvent. All reactions were conducted under a flow of nitrogen.

Procedure for Microwave Synthesis. Lead acetate is dissolved in the ethylene glycol by gentle heating in the microwave oven for approximately 1 min. Stoichiometric quantities of Te or Se powder are then added. The system is purged for a few minutes with nitrogen and then the microwave reactor is turned on. The reactions were conducted for 1 h.

Procedure for Ultrasonic Reaction. The procedure is the same as that in the microwave reaction, the only difference being that instead of a microwave oven, a sonicator is used. The reaction flask is gently water-cooled to prevent evaporation of the solvent. The reactions were conducted for 2 h.

(27) Fievet, F.; Lagier, J. P.; Figlarz, M. *MRS Bull.* **1989**, Dec, 29.
(28) Viau, G.; Fievet-Vincent, F.; Fievet, F. *J. Mater. Chem.* **1996**, *6*, 1047.
(29) Viau, G.; Fievet-Vincent, F.; Fievet, F. *Solid State Ionics* **1996**, *84*, 259.
(30) Sub, S.; Murray, C. B.; Weller, D.; Folks, L.; Moser, A. *Science* **2000**, *287*, 1989.
(31) Chow, G. M.; Kurihara, K. L.; Ma, D.; Feng, C. R.; Schoen, P. E.; Martinez-Miranda, L. J. *Appl. Phys. Lett.* **1997**, *70*, 2315.
(32) Bonet, F.; Guery, C.; Guyromard, D.; Herrera Urbina, R.; Tekaia-Elhsissen, K.; Tarascon, J.-M. *Int. J. Inorg. Mater.* **1999**, *1*, 47.
(33) Whittaker, A. G.; Mingos, D. M. P. *J. Chem. Soc.-Dalton Trans.* **2000**, 1521.
(34) Mason, T. J. *Sonochemistry: The Uses of Ultrasound in Chemistry*; Royal Society of Chemistry: Cambridge, 1990.
(35) Stadelmann, P. *Ultramicroscopy* **1987**, *131*.

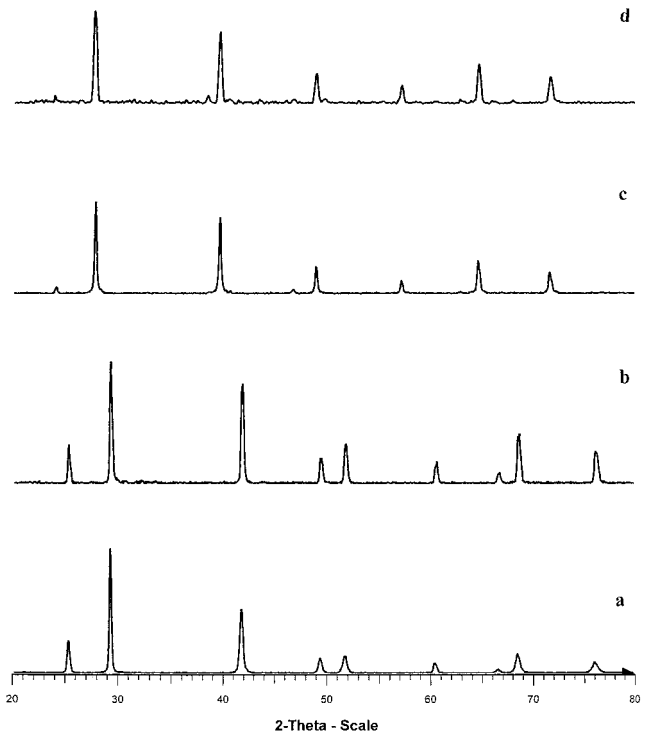

Figure 1. XRD patterns of (a) PbSe(mw), (b) PbSe(sono), (c) PbTe(mw), and (d) PbTe(sono).

The postreaction treatment procedure is the same for both methods, namely, centrifugation one time with the mother liquid, and a few times with EtOH, at 20 °C, 8000 rpm. Drying is under vacuum overnight.

Results and Discussions

To study the nature and morphology of the resulting product, techniques such as powder XRD, TEM, HR-TEM, SEM, EDX, DSC, elemental analysis (carbon), and FT-IR were employed.

The results of the powder XRD analysis are shown in Figure 1a−d. The sonochemical and the microwave-assisted methods yield the same solid phases for PbSe and PbTe. We have observed the formation of the pure Clausthalite phase for PbSe (PDF #06-0354) and the Altaite phase for PbTe (PDF #38-1435). The only difference between the two methods is found in very small impurities of unreacted Te (PDF #36-1452) that have been detected in the as-prepared sonochemical product of the PbTe synthesis. In both reactions, in the two methods, highly crystalline products are obtained. This is specially surprising for the sonochemical product, where in numerous cases amorphous or semicrystalline products are obtained due to the fast cooling rate that does not allow crystallization of the products.[36−42] The intensities and positions of the peaks are in very good agreement with literature values. Both products have a rock-salt (NaCl) cubic structure. The results of the calculation of the crystallite sizes employing the Scherrer equation are shown in Table 1.

Table 1. Reaction Conditions with Evaluations of the Particles Dimensions Obtained from TEM and XRD Measurements, Elemental Ratio from EDS, and Carbon Level in All Prepared Compounds

name of the compd	method of prepn	dimensions from XRD (nm)	dimensions from TEM (nm)	elemental ratio from EDS (Pb:chalcogen)	carbon level (%)
PbSe	mw	34.4	15−25	1.32:1	0.1029
PbSe	sono	36	31 × 18	1.13:1	0.04
PbTe	mw	45	30	1.1:1	0.058
PbTe	sono	29.7	11.2 × 10.3	1:1.27	0.068

TEM micrographs of the PbSe and PbTe from sonochemical (sono) and microwave (mw) reactions are presented in Figure 2a−f. Figure 2a,b depicts well-shaped rectangles of PbSe obtained by the sonochemical method; their crystallinity and crystallography is proven by selected area electron diffraction. A low level of aggregation is detected for these particles, and these aggregates further decompose to individual fine grains under the electron beam. Higher magnification of these particles reveals that some of them are partially elongated rectangles (see Figure 2b). The mean dimensions of these species are calculated from TEM micrographs by averaging over a few hundred species. The values obtained are as follows: length, 31 nm; width, 18 nm. The TEM micrographs of the PbSe obtained by the microwave synthesis is shown in Figure 2c. Spherical aggregates with average dimensions in the range 50−100 nm are observed. A closer observation of these aggregates reveals that they are built from 15−25-nm-sized aggregated particles. Figure 2d demonstrates the TEM images of the PbTe obtained from the sonochemical synthesis. Similar to the observation of PbSe(sono), nonagglomerated rectangles of PbTe are also detected. The mean dimensions of these particles calculated from TEM pictures are 11.2 × 10.3 nm. The PbTe particles were less elongated and much smaller than the PbSe (sono) particles. The structure of PbTe product obtained from the microwave synthesis is shown in Figure 2e. We have also obtained particles with rectangular shapes having a face length of approximately 30 nm. Unlike the sonochemical products, the particles were aggregated in a complex fractal structure. It is possible to detect in this picture rectangular "kinks" and stairs. We have further investigated the structure of PbTe(mw) by using HRTEM. The resulting micrograph is depicted in Figure 2f. The perfect NaCl structure is observed; the zone axis is [200] with *d* values between planes equal to 3.233 Å. This result is in agreement with HRTEM image simulations. Electron diffraction patterns for all these compounds are in good agreement with the XRD data. In Table 1 a comparison between the particle dimensions observed by TEM and calculated by XRD is presented. The general features deducted from the table are that the TEM observed size is smaller than the Scherrer calculated size. We attribute the relatively

(36) Ramesh, S.; Felner, I.; Koltypin, Y.; Gedanken, A. *J. Mater. Res.* **2000**, *15*, 944.
(37) Ramesh, S.; Sominska, E.; Cina, B.; Chaim, R.; Gedanken, A. *J. Am. Ceram. Soc.* **2000**, *83*, 89.
(38) Rojas, T. C.; Sayagues, M. J.; Caballero, A.; Koltypin, Y.; Gedanken, A.; Ponsonnet, L.; Vacher, B.; Martin, J. M.; Fernandez, A. *J. Mater. Chem.* **2000**, *10*, 715.
(39) Shafi, K.; Gedanken, A.; Prozorov, R.; Revesz, A.; Lendvai, J. *J. Mater. Res.* **2000**, *15*, 332.
(40) Wizel, S.; Margel, S.; Gedanken, A. *Polym. Int.* **2000**, *49*, 445.
(41) Zhong, Z. Y.; Mastai, Y.; Salkar, R. A.; Koltypin, Y.; Gedanken, A. *J. Mater. Res.* **2000**, *15*, 393.
(42) Kumar, R. V.; Koltypin, Y.; Cohen, Y. S.; Cohen, Y.; Aurbach, D.; Palchik, O.; Felner, I.; Gedanken, A. *J. Mater. Chem.* **2000**, *10*, 1125.

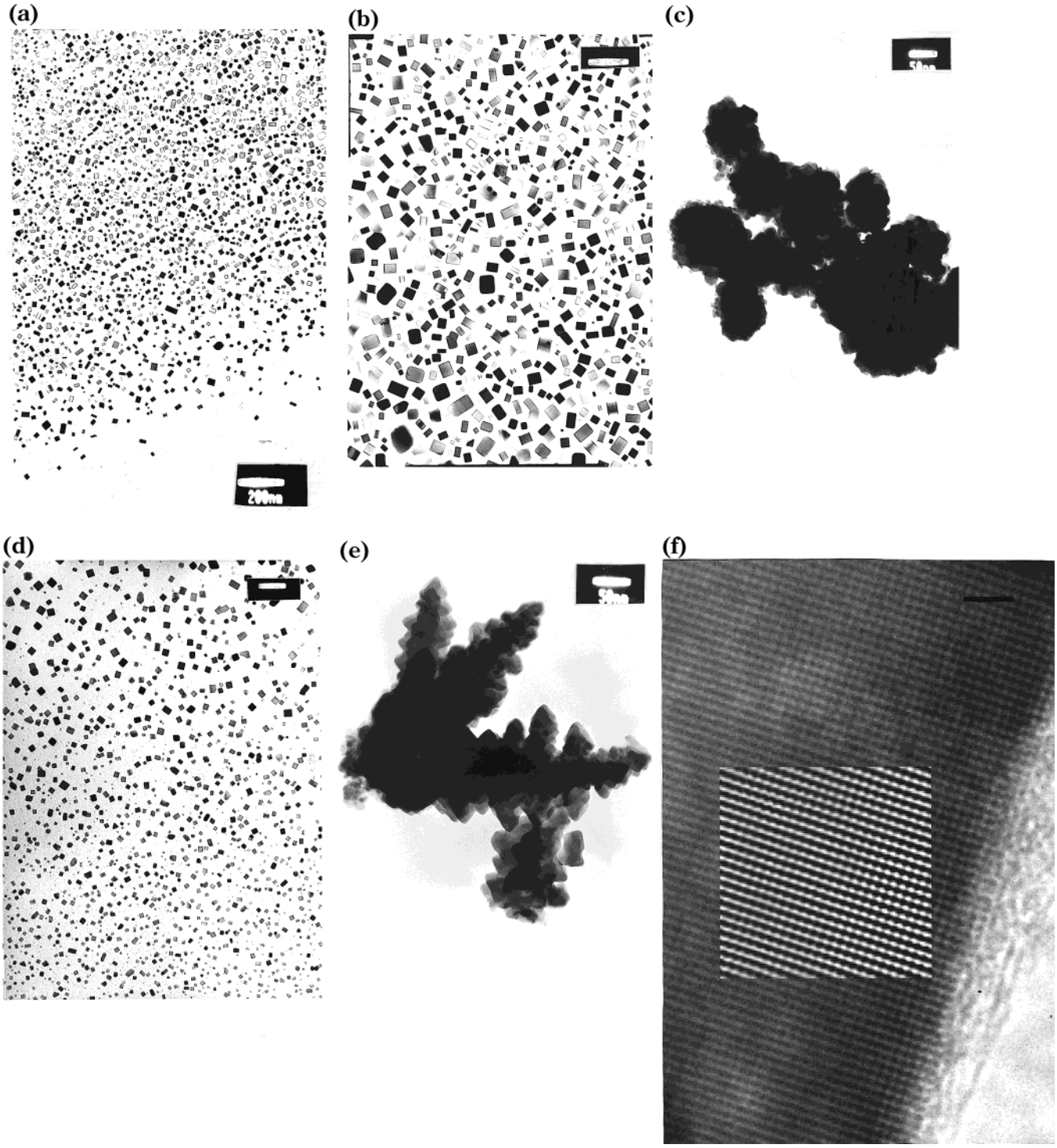

Figure 2. TEM pictures of (a) PbSe(sono) (bar equal to 200 nm), (b) PbSe(sono) higher magnification (bar equal to 100 nm), (c) PbSe(mw) (bar equal to 50 nm), (d) PbTe(sono) (bar equal to 50 nm), (e) PbTe(mw) (bar equal to 50 nm), and (f) HRTEM image of PbTe(mw) (bar equal to 32.3 Å), zone axis [200].

larger sizes of the XRD as originating from the internal strain in the products. This strain causes the broadening of XRD diffraction peaks without being reflected in the true dimensions. The existence of the strain is also demonstrated in the DSC measurements.

The stoichiometric ratios between the elements composing the as-prepared products are evaluated using EDX measurements and are presented in Table 1. In all cases the measured stoichiometric values are close to the expected theoretical 1:1 ratio, with some excess of Pb. An exception is obtained for PbTe (sono) where an excess of Te is measured. This excess can also be observed in the XRD data in Figure 1d where small Te diffraction peaks are observed.

Because of the high temperatures that developed in the sonochemical process as well as in the microwave-assisted reaction, it is always suggested that an elemental analysis be performed to learn about the extent of the solvent involvement in the reaction. The carbon analysis conducted reveals a very low level of carbon impurities (<0.08%) in all samples. This is another demonstration of the absence of arcing on the surface

of nanoparticles in microwave-assisted reactions. It is worth reporting that when following the microwave reaction we could not observe any discharge in the reaction cell. This observation contradicts early reports on the polyol synthesis of metals where a layer of chemisorbed ethylene glycol has been anchored on the surface of the product.[43] The FT-IR measurements (not shown here) also (not shown here) failed to reveal the presence of any chemisorbed ethylene glycol moieties. This result was further confirmed by temperature-programmed desorbtion mass spectroscopy (TPD-MS). We were unable to identify any organic residue desorbed from the surface of the powders when the temperature was raised to 400 °C.

To compare the morphology of the as-prepared selenides and tellurides, we have carried out SEM studies. Polydispersed aggregates of PbSe(sono), shown in Figure 3a, reveal spherical or rectangular shapes in the SEM image. The dimensions of these aggregates are 0.2−1 μm. Especially intriguing is the presence of aggregates with rectangular shapes because they look like cubic monocrystals of PbSe. This kind of aggregate is not observed in our TEM measurements despite the identical sample preparations in both cases. In the case of PbTe(sono) we observed smaller aggregates of particles (∼100−300 nm), and the shapes of these were mainly spherical. A discrepancy between SEM and TEM images is observed also for PbTe. SEM micrograph of the PbSe(mw) (see Figure 3b) reveals aggregates of nanoparticles with a mean radius <100 nm. In this case there is a good correlation between the TEM and SEM results. The PbTe(mw) image depicts aggregates with spongelike morphology.

To study the thermal properties of the as-prepared compounds, DSC analyses were conducted. The DSC examined the thermal stability of the powders. In all cases a few heating runs were performed. For the PbTe(sono) (see Figure 4a) an exothermic peak at ∼305 °C is observed. This peak disappears when the sample is cooled to room temperature and reheated in the same temperature range. The presence of such an exothermic transition may be result of the release of internal strain energy due to mechanical influences of ultrasound.[44] This stored energy is released in the form of an external thermal effect. Two endothermic peaks at ∼408 and ∼440 °C are related to the eutectic transition between PbTe and Te and to the transition PbTe + L → PbTe. These thermal effects, perhaps, reflect the fact that the resulting PbTe(sono) is enriched in unreacted Te. These results are in very good agreement with XRD (see Figure 1d) and EDX results (see table). Comparison of this result with DSC analysis of PbTe(mw) (see Figure 4b) did not reveal the exothermic peak at 305 °C, which has been assigned to a strain release process. Instead, only very small endothermic peaks are observed. They are assigned as proposed for the same endothermic peaks observed for PbTe(sono). (No free Te was observed in the XRD measurements because of the very weak sensitivity of this method to low-level impurities.) In the case of PbSe(sono) (see Figure 4c), we measure a very small endothermic peak (<11 mJ) observed at 220 °C. This peak corresponds to the eutectic reaction PbSe + Se → PbSe + liquid. This would require the observation of a very small impurity of Se, which is undetectable in the XRD measurements. On the contrary, the EDX spectrum shows a small excess of Pb. This endothermic peak is also present in the DSC spectrum of PbSe(mw). An exothermic peak at 405 °C is observed (for PbSe(sono)); however, we cannot assign this peak without further experimentation. This exothermic peak is not detected in the DSC spectrum of PbSe(mw) (see Figure 4d).[45] The endothermic peaks at 440 °C (PbTe) and 220 °C (PbSe) disappear when the heated sample is cooled and reheated. The disappearance of these peaks, which occur at the melting temperatures of Te and Se, respectively, is due to their small amounts. They evaporate and are carried out by the argon (or N_2) carrier.

Discussion

We consider the low level of carbon impurities in the sonochemical as well as in the microwave-assisted reactions as the most dramatic result in this study. This is especially surprising for the sonochemical reaction. Results that have been obtained for close to 100 sonochemical products in which organic solvents or organic precursors were involved always show 1−2 wt % of carbon. This is due to the extreme conditions of the sonochemical reaction, which result in the decomposition of organic solvents. On this basis, it is expected that residues of ethylene glycol will be found as impurities in the product. This will happen only if the bubble indeed develops to its full capacity and efficient collapse takes place. Moreover, it is expected that since the final temperature reached after the collapse of the bubble is inversely proportional to the vapor pressure of the solvent, and since ethylene glycol has a relatively low vapor pressure, very high temperatures will result as the bubble collapses. However, we have to take into account that perhaps because of the high viscosity of ethylene glycol and the hydrogen bonds, a transient bubble will not develop under these conditions. In other words, to separate ethylene glycol molecules and to form a cavity will require a much higher threshold than those for water, decane, Decalin, or other favorite solvents. It is therefore possible that the current reaction is a thermal and not a sonochemical reaction. To check this hypothesis, we have carried out the reaction at 200 °C without ultrasonic waves. Indeed, the expected sellenide and tellurides were obtained. However, the products were approximately 800-nm- to 1-μm-sized particles. Another control reaction was sonochemistry at 10 °C, which has not yielded products. This is further proof of the fact that temperature is a driving force for such reactions. This leads to the conclusion that moderate temperatures are required for the reaction. However, although the reaction yielded products when carried out at 200 °C, the nanosized particles obtained when ultrasound radiation is applied indicate the involvement of bubbles in the process. Nanoparticles are a typical product of a sonochemical reaction. Our interpretation

(43) Hegde, M. S.; Larcher, D.; Dupont, L.; Beaudoin, B.; Tekaia-Elhsissen, K.; Tarascon, J.-M. *Solid State Ionics* **1997**, *93*, 33.

(44) Bouad, N.; Marin-Ayral, R. M.; Tedenac, J. C. *J. Alloys Compd.* **2000**, *297*, 312.

(45) Massalski, T. B.; Okamoto, H. *Binary Alloys Phase Diagrams*, 2nd ed.; ASM International: Materials Park, OH, 1996.

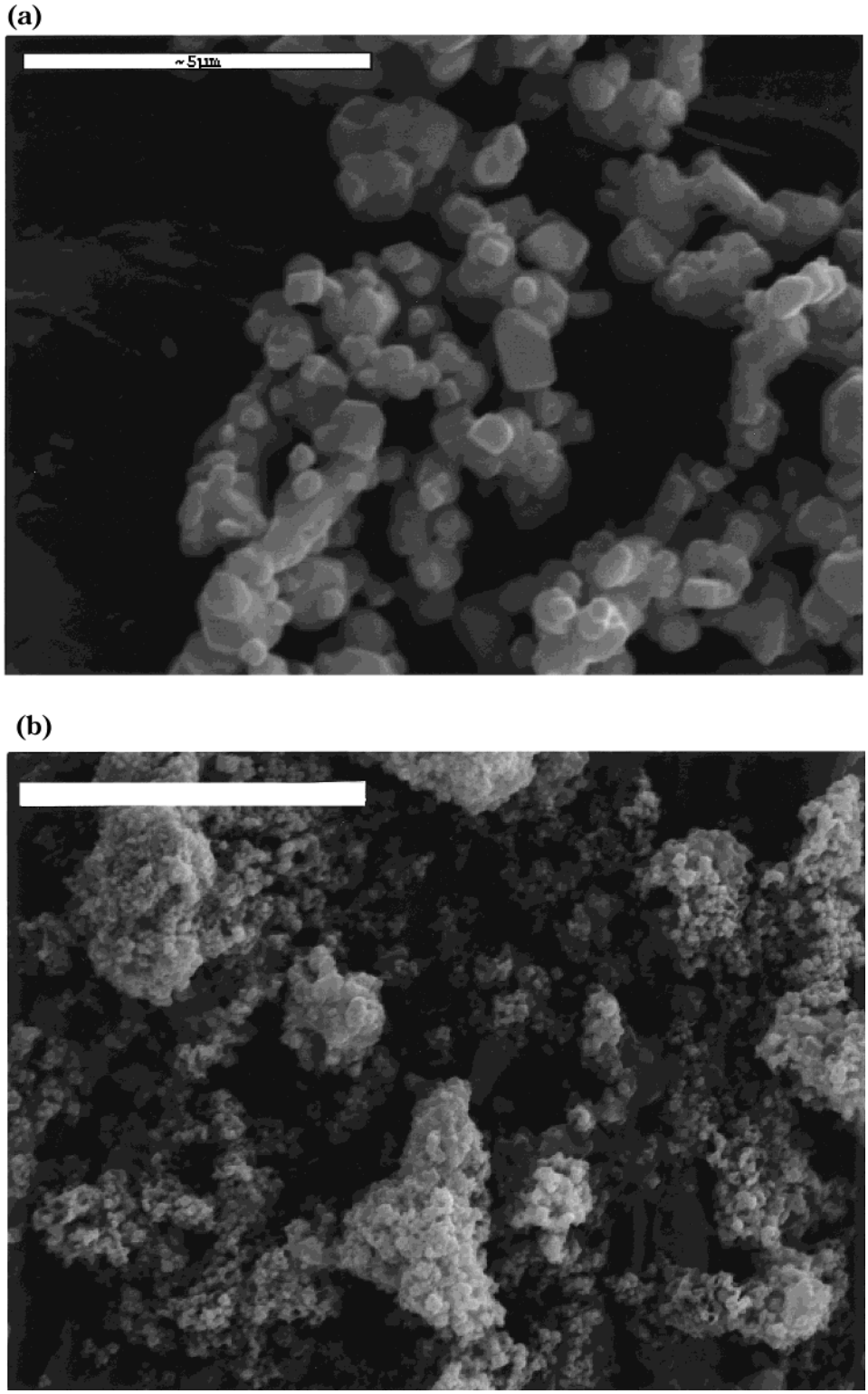

Figure 3. SEM images of (a) PbSe(sono) (bar equal to 5 μm) and (b) PbSe(mw) (bar equal to 1 μm).

for the small percentage of carbon impurities is that cavities are being formed, but grow only slightly. When they collapse, a relatively low temperature is obtained. At this moderate temperature ethylene glycol does not decompose.

The low level of contaminants is detected not only in the sonochemical products but also in the products of the mw-assisted reactions. This is also considered as a surprise because it is expected that as a result of the arcing phenomenon occurring during the mw reaction the rupture of the solvent's chemical bonds will be facilitated, thus increasing the contamination level. The arcing is usually explained as originating from the interaction of the metallic nanoparticle with microwave radiation. If the reaction would have been conducted under oxygen, we could explain the low level of carbon as resulting from the formation of CO_2. However, our reactions are carried out under argon, which cannot explain the lack of carbon contamination. The arcing of metal powders in liquid systems has been the center of

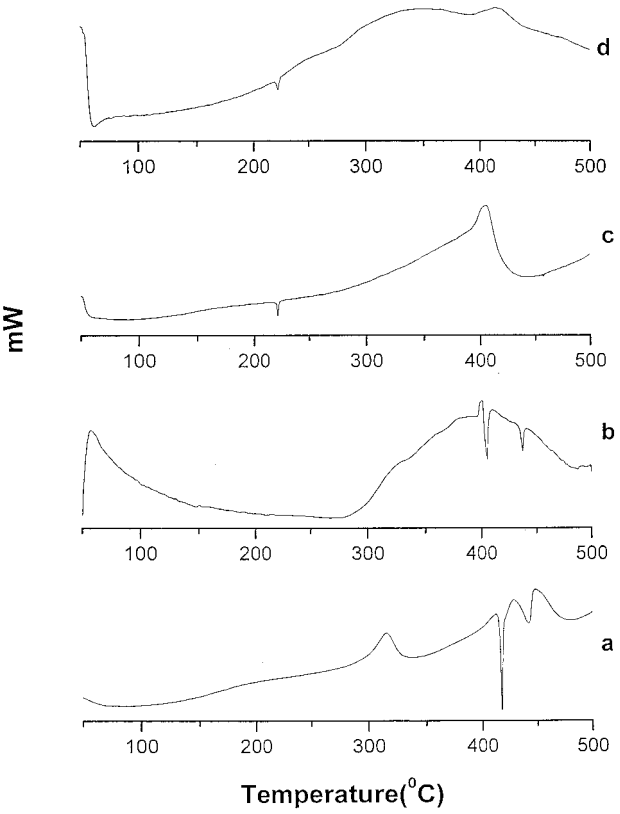

Figure 4. DSC curves of (a) PbTe(sono), (b) PbTe(mw), (c) PbSe(sono), and (d) PbSe(mw).

a recent study by the group of Mingos.[33] We will adopt few of the arguments mentioned in their manuscript for the current case, although the two systems differ considerably. The reasons for absence of a discharge during the formation of the metallic particles can be explained as follows: (1) the discharge is formed between the metallic particles, and due to the low concentration of the particles in the solvent, it does not occur. The metallic nanoparticles are intermediate products in the reaction and their instantaneous concentration is always small. (2) The nanosize of the metallic particles formed does not favor arcing. (3) The high boiling point of the solvent does not support arcing. (4) Preliminary results of a kinetic study of this reaction show that while the formation of the Pb is a slow process, its reaction with Te is very fast. This might be another reason for the absence of arcing.

Another interesting point is the difference in the morphology and microstructure of the products obtained using microwave-assisted chemistry as compared with that obtained sonochemically. The products of the microwave reaction were more aggregated than those obtained sonochemically. In fact, their mode of aggregation resembles the products of classical solid-state reactions. The interpretation will follow our previous argument that undeveloped cavities are collapsing. In the sonochemical reaction the number of crystalline seeds associated with each collapsing bubble is small, and although the temperature might be higher than the MW reaction, aggregation is reduced. It is also possible that the strong stirring of the solution also prevents aggregation.

The mechanism of the formation of the particles is still under investigation but already at this stage we know some of the conditions in order for such a reaction to succeed. For example, the reagent must be both soluble in ethylene glycol and independently reducible by the solvent.

In summary, we have presented the microwave and ultrasonically assisted polyol synthesis of the PbSe and PbTe. Both products were obtained in nanometric dimensions, with different morphologies, and very low levels of carbon impurity. Possible explanations for such low levela of C impurities and mechanisms for the formation of the nanoparticles are presented.

Acknowledgment. This work was supported by the Bar-Ilan research and development authorities. The authors are grateful to Prof. Z. Malik of the Department of Life Sciences for extending the use of their facilities to us. Prof. W. Kaplan and J. Josef of the Department of Material Engineering, Technion, for their assistance in HRTEM measurements. O. Palchik gratefully acknowledges Y. Epstein for useful discussions. R. Kerner thanks M. Harpeness for useful advice.

CM001411H